

High-sensitivity SrTiO₃ photodetectors with paralleled multiple interdigital electrode cells

Le Wang, Kui-juan Jin,* Jie Xing, Chen Ge, Hui-bin Lu,
Wen-jia Zhou, and Guo-zhen Yang

Beijing National Laboratory for Condensed Matter Physics, Institute of Physics,
Chinese Academy of Sciences, Beijing 100190, China

*Corresponding author: kjjin@iphy.ac.cn

Received 14 January 2013; revised 29 March 2013; accepted 19 April 2013;
posted 19 April 2013 (Doc. ID 183473); published 14 May 2013

We report high-sensitivity SrTiO₃ photoconductive detectors with multiple photoelectric cells connected in parallel. The photocurrent of the detectors increases significantly with an increase of the cell number. The photocurrent responsivity of the detector with three cells can reach 237 mA/W at 10 V bias under illumination of the 375 nm laser, and the corresponding quantum efficiency is 77% at 10 V bias. Furthermore, a transient photovoltaic signal with a rise time of ~490 ps and a full width at half-maximum of ~900 ps is obtained. These results demonstrate that the present devices with further improvement of performance have great potential application in high-sensitivity and ultrafast ultraviolet photodetectors. © 2013 Optical Society of America

OCIS codes: (040.5160) Photodetectors; (040.5150) Photoconductivity; (040.7190) Ultraviolet; (320.5390) Picosecond phenomena.

<http://dx.doi.org/10.1364/AO.52.003473>

1. Introduction

Ultraviolet (UV) photodetectors with excellent thermal stability and reliability have drawn a great deal of interest in recent years due to their various potential applications in the fields of solar astronomy, short-range communications security, biological research, fire alarms, and military services [1–4]. Conventional semiconductors such as silicon and gallium arsenide can be used in UV detection, but they exhibit poor radiation hardness and have high dark currents with increasing bias owing to their narrow bandgap [5]. Perovskite oxides have attracted considerable attention due to their abundant properties, such as dielectric, piezoelectric, ferroelectric, ferromagnetic, superconducting, optical characteristics, and photoelectric effect [6–8]. Recently, we have reported the visible-blind or solar-blind UV photodetectors based on perovskite oxide single crystals with

wide bandgaps, including SrTiO₃ (STO) [9,10], LaAlO₃ [11], LiNbO₃ [12], and LiTaO₃ [13], with Au interdigitated electrodes. These photodetectors based on perovskite oxide single crystals have high UV sensitivities and low dark currents [9–13]. In this paper, we present high-sensitivity SrTiO₃ photodetectors by fabricating an interdigital electrode cell array on the surface of a SrTiO₃ single crystal. One important part of our work is that it can reduce the difficulty of large-area lithography and facilitate integration. The photocurrent of the photodetector can increase significantly with the cell number without the need for an amplifier or high-precision instrument, as we can integrate multiple cells on the detector in parallel configuration. In addition, the response speed of our STO photodetector with multiple interdigital electrode cells connected in parallel is faster than before [10].

2. Experimental Details

The STO single crystal used in this paper is the commercial single polished STO (001) single crystal

with a purity of 99.99%. The size of the STO wafer is 10 mm × 10 mm with a thickness of 0.5 mm. Figure 1(a) shows the schematic diagram of our STO photodetector with four interdigitated electrode cells. A Ti layer with a thickness of 20 nm was deposited onto the surface of the STO, and then an Au layer with a thickness of 100 nm was deposited onto the Ti layer by thermal evaporation. UV lithography and etching were performed to fabricate the interdigitated electrodes. The finger width and the interspacing of the interdigitated electrodes are both 10 μm. Due to the shadowing effect of electrodes, the irradiated active area of one interdigitated electrode cell is 0.086 mm². Multiple interdigitated electrode cells can be connected in parallel using conductive silver epoxy in measurement. A tunable DC voltage source (Keithley 2400) was taken as the bias supply V_b . The photoelectric properties of our photodetectors were investigated under the irradiation of an incandescent lamp, a continuous blue laser (Oxxius, wavelength of 375 nm), and a Nd:YAG pulsed laser (wavelength of 355 nm).

3. Results and Discussion

Figure 1(b) shows the I - V characteristics of the photodetector with one cell and three cells in the dark and under illumination of an incandescent lamp. From Fig. 1(b), it can be seen that the photocurrent of the STO photodetector with three cells is larger than that of the STO photodetector with one cell at the same V_b . The mechanism of photocurrent for the STO photodetectors with interdigitated electrodes can be easily understood as the following: the STO absorbs the incident photons and generates the photocarriers, when the photon energies are higher than the bandgap of STO (~ 3.2 eV) [14]. The photogenerated

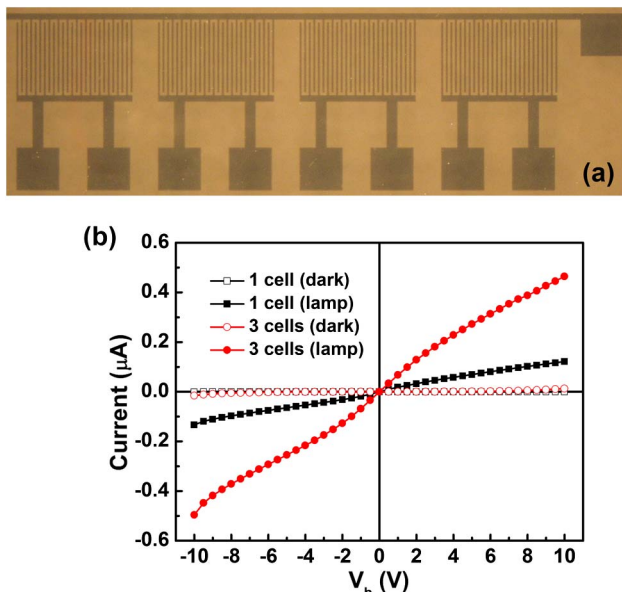


Fig. 1. (a) Schematic diagram of the STO photodetector with four interdigitated electrode cells. (b) Comparison of I - V characteristics measured in dark and under illumination of an incandescent lamp.

electrons and holes are separated by the electric field of supplied bias, and then the photocurrent forms [10].

Figure 2(a) shows the voltage dependence of photocurrents for the STO photodetector with multiple cells under illumination of a 375 nm laser. At a fixed power density of 1.23 mW/cm², the photocurrent increases linearly with the applied bias. It is easy to understand that a larger V_b will provide a higher electric field as a driving force to separate the photocarriers more efficiently. The recombination of photocarriers will be reduced, and more carriers can be collected. Thus, the photocurrent of the photodetector increases linearly with V_b . We also measured the dark currents of the photodetector, as shown in Fig. 2(a). The dark current of the STO photodetector will increase sharply when the absolute value of the bias voltage is larger than 30 V (not shown here), which will lead to the reduction of the detector's signal-to-noise ratio. Figure 2(b) shows the dependence of the currents on the cell number measured in the dark and under illumination of an incandescent lamp or a 375 nm laser at 10 V bias. From Fig. 2(b), it can be seen that the photocurrent increases with the cell number at the same bias voltage due to the influence of the parallel circuit.

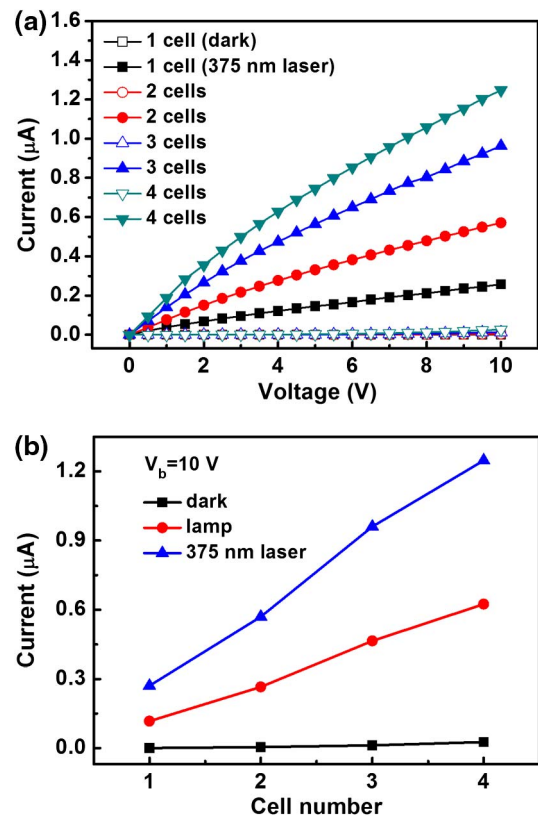


Fig. 2. (a) Voltage dependence of currents in the devices with different interdigitated electrode cell numbers. Open data points are for dark currents and solid data points indicate photocurrents under illumination of a 375 nm laser. (b) Interdigitated electrode cell number dependence of currents measured in dark and under illumination of an incandescent lamp or a 375 nm laser at 10 V bias. The power density of the 375 nm laser is 1.23 mW/cm².

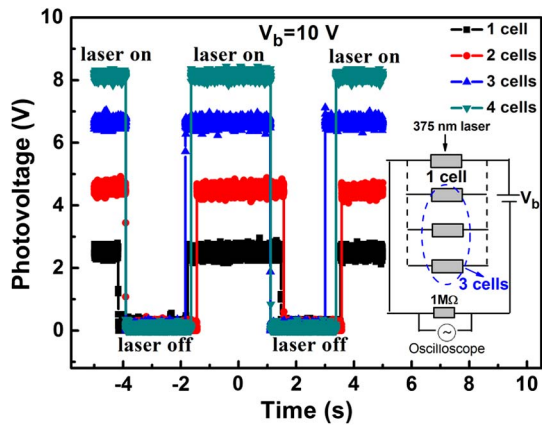


Fig. 3. Steady-state photovoltaic response of the devices with different interdigitated electrode cell numbers under illumination of a 375 nm laser at 10 V bias. The power density is 10 mW/cm². The inset shows the schematic circuit of measurement.

The steady-state photovoltaic properties of the devices with multiple cells were studied under illumination of the 375 nm laser, as shown in Fig. 3. The inset shows the schematic circuit of the measurement. The photovoltaic signals were recorded by an oscilloscope with a 2.5 GHz bandwidth and an input impedance of 1 MΩ. The power density is 10 mW/cm², and the bias was 10 V. From Fig. 3, it can be seen that the photovoltage is high (low) when the 375 nm laser is on (off), and the photovoltage increases from 2.4 to 8.1 V when the cell number increases from 1 to 4.

Figure 4 shows the dependence of the photocurrent of the STO photodetector on the power density of a 375 nm laser at 10 V bias. The photocurrent has a good linear relationship with the power density, and no photocurrent saturation phenomenon occurs in the power density range of 0–70 mW/cm². The photocurrent responsivity R_i was calculated by [15]

$$R_i = \frac{I}{A_{\text{eff}}E}, \quad (1)$$

where I is the photocurrent, A_{eff} is the active area of the device, and E is the irradiance of the light.

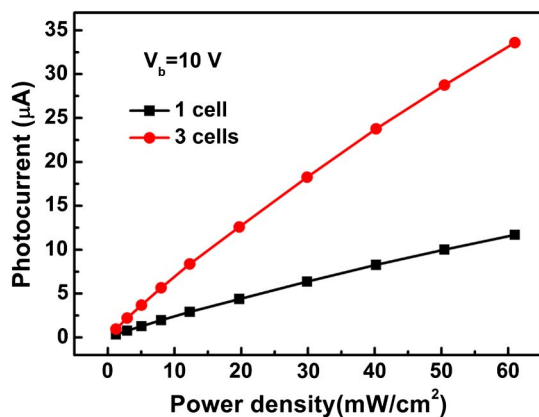


Fig. 4. Variation of photocurrent with laser power density at 10 V bias.

Under illumination of the 375 nm laser (power density 30 mW/cm²), a photocurrent responsivity of 237 mA/W is obtained for three cells at 10 V bias. The corresponding quantum efficiency η for three cells is 77% at the bias of 10 V according to

$$\eta = \frac{R_i h\nu}{q}, \quad (2)$$

where R_i is the photocurrent responsivity of the photodetector, h is the Planck constant, ν is the frequency of incident light, and q is the charge of the electron. Here, we did not consider the incident light on the electrodes. In our current devices, the open area is almost equal to the area covered by the electrodes because the finger width and the interspacing of the interdigitated electrodes are both 10 μm. By adjusting the parameters of the interdigitated electrode, for example, by reducing the finger width, we think it will be possible to have much larger open area and further improve the device performance. The photocurrent responsivity and the corresponding quantum efficiency of our photodetector are comparable or even better than those of many other UV detectors based on semiconductors [16–18]. Compared with photodetectors reported previously [9–13], the main advantage of our STO photodetector is the interdigitated electrode cell array; thus the photocurrent can be enhanced and tunable.

In addition, we also measured the temporal response of our devices at 10 V bias using a 355 nm actively passively mode-locked Nd:YAG laser with 15 ps duration. The energy density is 1.5 mJ/cm². To reduce the influence of the measurement circuit, we connected a 0.5 Ω resistance in parallel with the device. As shown in Fig. 5, the detector with one cell has a rise time of ~330 ps and a full width at half-maximum (FWHM) of ~600 ps. Moreover, the detector with three cells in parallel has a rise time of ~490 ps and a FWHM of ~900 ps. Measurements on devices with different cell numbers showed that the temporal responses of our detectors were related to the size of the devices, and a smaller device should

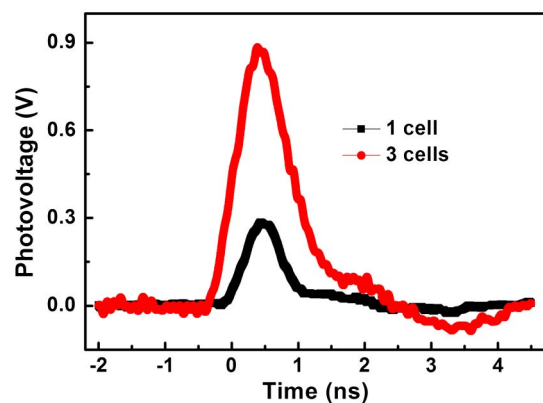


Fig. 5. Temporal photovoltaic response of the devices under the excitation of a 355 nm pulsed laser with 15 ps duration. The energy density is 1.5 mJ/cm².

have a faster response speed due to the reduced capacitance and RC time constant. Thus, the measured rise time of the detector with one cell is faster than that of the detector with three cells. The response speeds of the device with one cell and with three cells are still faster than the results of previously reported photodetectors [10]. The variation of the photovoltages with different energy density was also studied. The timing characteristics, such as the rise time and FWHM, remain almost unchanged. This indicates that the timing characteristics are the essential characteristics of the device and are not related to the energy density, which is important for device applications.

4. Conclusions

In summary, we have fabricated high-sensitivity STO photodetectors based on an interdigital electrode cell array. The photocurrent of the detector can increase significantly with an increase of the cell number, as we can integrate multiple cells on the detector in parallel configuration. Moreover, the present STO photodetectors have a high photocurrent responsivity of 237 mA/W at 375 nm at 10 V bias and an ultrafast response time of hundreds of picoseconds.

This work is supported by the National Basic Research Program of China (Nos. 2012CB921403 and 2013CB328706) and the National Natural Science Foundation of China (Nos. 10825418 and 11134012). The authors also thank Y. N. Hou for his help with UV lithography and etching.

References

1. H. Ohta and H. Hosono, "Transparent oxide optoelectronics," *Mater. Today* **7**(6), 42–51 (2004).
2. H. Jiang and T. Egawa, "High quality AlGa_N solar-blind Schottky photodiodes fabricated on AlN/sapphire template," *Appl. Phys. Lett.* **90**, 121121 (2007).
3. T. Tut, T. Yelboga, E. Ulker, and E. Ozbay, "Solar-blind AlGa_N-based p-i-n photodetectors with high breakdown voltage and detectivity," *Appl. Phys. Lett.* **92**, 103502 (2008).
4. Y. Zhang, S.-C. Shen, H. J. Kim, S. Choi, J.-H. Ryou, R. D. Dupuis, and B. Narayan, "Low-noise GaN ultraviolet p-i-n

- photodiodes on GaN substrates," *Appl. Phys. Lett.* **94**, 221109 (2009).
5. M. Razeghi and A. Rogalski, "Semiconductor ultraviolet detectors," *J. Appl. Phys.* **79**, 7433–7470 (1996).
6. R. Cauro, A. Gilabert, J. P. Contour, R. Lyonnet, M. G. Medici, J. C. Grenet, C. Leighton, and I. K. Schuller, "Persistent and transient photoconductivity in oxygen-deficient La_{2/3}Sr_{1/3}MnO_{3-δ} thin films," *Phys. Rev. B* **63**, 174423 (2001).
7. Z. G. Sheng, Y. P. Sun, J. M. Dai, X. B. Zhu, and W. H. Song, "Erasure of photoconductivity by magnetic field in oxygen-deficient La_{2/3}Sr_{1/3}MnO_{3-δ} thin films," *Appl. Phys. Lett.* **89**, 082503 (2006).
8. X. Yuan, Z. J. Yan, Y. B. Xu, G. M. Gao, K. X. Jin, and C. L. Chen, "Switching behavior of oxygen-deficient La_{0.6}Ca_{0.4}MnO_{3-δ} thin films," *Appl. Phys. Lett.* **90**, 224105 (2007).
9. K. Zhao, K. J. Jin, Y. H. Huang, S. Q. Zhao, H. B. Lu, M. He, Z. H. Chen, Y. L. Zhou, and G. Z. Yang, "Ultraviolet fast-response photoelectric effect in tilted orientation SrTiO₃ single crystals," *Appl. Phys. Lett.* **89**, 173507 (2006).
10. J. Xing, K. Zhao, H. B. Lu, X. Wang, G. Z. Liu, K. J. Jin, M. He, C. C. Wang, and G. Z. Yang, "Visible-blind, ultraviolet sensitive photodetector based on SrTiO₃ single crystal," *Opt. Lett.* **32**, 2526–2528 (2007).
11. J. Xing, E. J. Guo, K. J. Jin, H. B. Lu, J. Wen, and G. Z. Yang, "Solar-blind deep-ultraviolet photodetectors based on an LaAlO₃ single crystal," *Opt. Lett.* **34**, 1675–1677 (2009).
12. E. J. Guo, J. Xing, K. J. Jin, H. B. Lu, J. Wen, and G. Z. Yang, "Photoelectric effects of ultraviolet fast response and high sensitivity in LaAlO₃ single crystal," *J. Appl. Phys.* **106**, 023114 (2009).
13. E. J. Guo, J. Xing, H. B. Lu, K. J. Jin, J. Wen, and G. Z. Yang, "Ultraviolet fast-response photoelectric effects in LaAlO₃ single crystal," *J. Phys. D* **43**, 015402 (2010).
14. H. Katsu, H. Tanaka, and T. Kawai, "Anomalous photoconductivity in SrTiO₃," *Jpn. J. Appl. Phys.* **39**, 2657 (2000).
15. X. Kong, C. Liu, W. Dong, X. Zhang, C. Tao, L. Shen, J. Zhou, Y. Fei, and S. Ruan, "Metal-semiconductor-metal TiO₂ ultraviolet detectors with Ni electrodes," *Appl. Phys. Lett.* **94**, 123502 (2009).
16. G. Ariyawansa, M. B. M. Rinzan, M. Alevli, M. Strassburg, N. Dietz, A. G. U. Perera, S. G. Matsik, A. Asghar, I. T. Ferguson, H. Luo, A. Bezinger, and H. C. Liu, "Ga_N/AlGa_N ultraviolet/infrared dual-band detector," *Appl. Phys. Lett.* **89**, 091113 (2006).
17. S. Butun, T. Tut, B. Butun, M. Gokkavas, H. Yu, and E. Ozbay, "Deep-ultraviolet Al_{0.75}Ga_{0.25}N photodiodes with low cutoff wavelength," *Appl. Phys. Lett.* **88**, 123503 (2006).
18. O. M. Nayfeh, S. Rao, A. Smith, J. Therrien, and M. H. Nayfeh, "Thin film silicon nanoparticle UV photodetector," *IEEE Photon. Technol. Lett.* **16**, 1927–1929 (2004).